

This discussion paper is/has been under review for the journal Atmospheric Chemistry and Physics (ACP). Please refer to the corresponding final paper in ACP if available.

Impacts of absorbing biomass burning aerosol on the climate of southern Africa: a Geophysical Fluid Dynamics Laboratory GCM sensitivity study

C. A. Randles^{1,*} and V. Ramaswamy^{1,2}

¹Atmospheric and Oceanic Sciences Program, Princeton University, Princeton, New Jersey, USA

²NOAA Geophysical Fluid Dynamics Laboratory, Princeton, New Jersey, USA

* now at: Goddard Earth Sciences and Technology Center, University of Maryland, Baltimore County and NASA GSFC Code 613.3, Greenbelt, Maryland, USA

Received: 19 February 2010 – Accepted: 25 March 2010 – Published: 16 April 2010

Correspondence to: C. A. Randles (cynthia.a.randles@nasa.gov)

Published by Copernicus Publications on behalf of the European Geosciences Union.

Biomass burning aerosol climate impacts

C. A. Randles and
V. Ramaswamy

Title Page

Abstract

Introduction

Conclusions

References

Tables

Figures

⏪

⏩

◀

▶

Back

Close

Full Screen / Esc

Printer-friendly Version

Interactive Discussion

Abstract

Tropospheric aerosols emitted from biomass burning reduce solar radiation at the surface and locally heat the atmosphere. Equilibrium simulations using an atmospheric general circulation model (GFDL AGCM) indicate that strong atmospheric absorption from these particles can cool the surface and increase upward motion and low-level convergence over southern Africa during the dry season. These changes increase sea level pressure over land in the biomass burning region and spin-up the hydrologic cycle by increasing clouds, atmospheric water vapor, and, to a lesser extent, precipitation. Cloud increases serve to reinforce the surface radiative cooling tendency of the aerosol. Conversely, if the climate over southern Africa were hypothetically forced by high loadings of scattering aerosol, then the change in the low-level circulation and increased subsidence would serve to decrease clouds, precipitation, and atmospheric water vapor. Warming from cloud decreases mitigates surface cooling associated with scattering-only aerosols.

1 Introduction

Biomass burning is a significant source of tropospheric aerosols in southern Africa during the dry season (August to October or ASO). These carbonaceous particles extinguish the amount of sunlight reaching the Earth's surface, and their absorbing black carbon (BC) component heats the atmosphere aloft. By directly redistributing solar heating between the atmosphere and surface, BC aerosols can impact atmospheric stability, regional circulation patterns, and the hydrologic cycle (Ramanathan and Carmichael, 2008).

The IPCC estimates the direct radiative forcing of biomass burning (bb) aerosol to be $+0.03 \pm 0.12 \text{ W m}^{-2}$ on the global, annual average (Solomon et al., 2007); however, it can be much greater than that of greenhouse gases (GHGs) on local and regional scales (e.g. Keil and Haywood, 2003). Much of the uncertainty in bb aerosol radiative

Biomass burning aerosol climate impacts

C. A. Randles and
V. Ramaswamy

Title Page

Abstract

Introduction

Conclusions

References

Tables

Figures

⏪

⏩

◀

▶

Back

Close

Full Screen / Esc

Printer-friendly Version

Interactive Discussion

forcing results from uncertainties in (1) the aerosol optical properties and (2) the spatial distribution of the aerosol in both the horizontal and vertical (e.g. Haywood and Ramaswamy, 1998). There is even greater uncertainty involved when trying to determine the response of the hydrologic cycle to bb aerosol forcing. Microphysical interactions between aerosols and clouds may impact precipitation formation processes (indirect effect). Shortwave atmospheric heating by absorbing aerosol may increase evaporation in cloud drops and reduce low-level clouds and precipitation while increasing column stability (semi-direct effect) (Johnson et al., 2004). In contrast, widespread regional aerosol atmospheric heating may induce rising motion and low-level moisture convergence that increases clouds, rainfall, and latent heating, the latter of which excites positive feedback processes (e.g. Lau et al., 2006; Randles and Ramaswamy, 2008 (hereafter RR08)). This increased rainfall, however, may be tempered or even eliminated once the aerosol surface radiative cooling tendency is manifest in sea surface temperature (SST) tendencies (e.g. Ramanathan and Charnichael, 2008).

Many studies have focused on quantifying the optical properties of and radiative forcing due to bb aerosols over southern Africa (e.g. Myhre et al., 2003; Abel et al., 2005), with widely ranging estimates of top-of-the-atmosphere (TOA), atmospheric (ATM) and surface (SFC) radiative forcing. Fewer studies have examined the climate response of the African region to bb aerosol forcing. Paeth and Feichter (2006) used equilibrium simulations in the ECHAM4 GCM to de-convolve the influences of GHGs and bb aerosol on climate. While GHG warming tended to dominate the surface air temperature response, they found that aerosol induced solar flux reductions to the surface contributed to an overall decrease in sensible and latent heat fluxes and precipitation in southern Africa. In contrast, using transient simulations in the Max Planck Institute Earth System Model (MPI-ESM), a fully coupled atmosphere-ocean GCM with interactive aerosols, Roeckner et al. (2006) found that GHG induced surface air warming over central Africa was largely compensated by bb aerosol cooling. Also, increased atmospheric absorption from larger increases in carbonaceous aerosols contributed to circulation changes that favored the transport of moisture from the Atlantic Ocean into

**Biomass burning
aerosol climate
impacts**C. A. Randles and
V. Ramaswamy

Title Page

Abstract

Introduction

Conclusions

References

Tables

Figures

◀

▶

◀

▶

Back

Close

Full Screen / Esc

Printer-friendly Version

Interactive Discussion

southern Africa and contributed to a positive impact on the overall precipitation trend. Though the results of these studies differ, they each demonstrate that bb aerosols likely impact climate in a significant manner in southern Africa.

In the present study, using an atmospheric general circulation model (AGCM), we investigate the sensitivity of the climate impacts by considering a wide range in bb aerosol forcing, which gives substantial additional perspectives relative to the aforementioned studies. We incorporate satellite and in situ measurements of two key column-integrated aerosol optical properties at 500 nm, the aerosol extinction optical depth (AOD) and the single scattering albedo (SSA), into some of these sensitivity experiments in an attempt to address uncertainties in bb aerosol radiative forcing. Our analysis is focused on the response of the southern African climate to bb aerosols, given that these aerosols are a significant part of the column burden and thus are likely to be a major aerosol player in the region. Special emphasis is placed on surface air temperature and precipitation responses.

2 Model description and experimental design

The analysis is based on experiments performed with the Geophysical Fluid Dynamics Laboratory's (GFDL) atmospheric-land GCM AM2-LM2 (Anderson et al., 2004) set to N45 resolution (2.5° longitude \times 2.0° latitude with 24 vertical levels). Ginoux et al. (2006) describe the treatment and evaluation of aerosols in the GCM. Briefly, three-dimensional monthly-mean mass profiles of five externally-mixed aerosol species (sulfate, BC, organic carbon (OC), dust, and sea salt) are simulated off-line with a chemical transport model and prescribed (linearly interpolated between months). Optical properties for each species are determined offline using Mie theory and assumed aerosol physical and optical properties (Haywood and Ramaswamy, 1998; Haywood et al., 1999). The optical effects of hygroscopic growth with changing model RH are considered for sea salt and sulfate aerosols. For this study, the optical properties of OC aerosols are modified to allow for mild absorption and hygroscopic growth following

Biomass burning aerosol climate impacts

C. A. Randles and
V. Ramaswamy

Title Page

Abstract

Introduction

Conclusions

References

Tables

Figures

⏪

⏩

◀

▶

Back

Close

Full Screen / Esc

Printer-friendly Version

Interactive Discussion

Ming et al. (2005) to be consistent with observations of bb aerosol hygroscopic growth from the southern African SAFARI 2000 field campaign (Magi et al., 2003). The model includes the direct and semi-direct aerosol effects only (i.e. aerosols impact radiative fluxes); interactions between aerosols and cloud microphysics are not considered.

Our experimental design is similar to Menon et al. (2002) and RR08, and it aims to isolate the climate response to a range of bb aerosol forcing. Table 1 summarizes the treatment of aerosols in each experiment, which we describe in more detail here. We conduct four sensitivity experiments, all of which share the same present-day climatological observed SSTs (Reynolds et al., 2002), sea-ice, long-lived GHGs, ozone, and land-surface properties. We run each equilibrium simulation for 35 years and analyze the results from the last 30 years and determine significance using a two-tailed student's t-test as in RR08. In the control experiment (CTRL), we prescribe natural (dust plus sea salt) and sulfate aerosol distributions simulated by the Model of OZone And Related chemical Tracers version 2 (MOZART-2) (Horowitz, 2006) for the year 2000; no carbonaceous aerosols (BC plus OC) are prescribed in this experiment. In experiment MOZEX, we also include BC and OC aerosols from MOZART-2. Magi et al. (2009) and Ginoux et al. (2006) both found that in biomass burning regions, modeled column-integrated AOD in AM2-LM2 tended to be biased low relative to observations from the ground-based AEROSol robotics NETwork (AERONET) (Holben et al., 2001) and retrievals from the NASA MODIS satellite (Kaufman et al., 1997). Discrepancies between modeled (low-biased) AOD and (high-biased) SSA relative to observations are minimized in AM2-LM2 by increasing OC and BC emissions by factors of 1.6 and 1.8, respectively (Magi et al., 2009).

Motivated by the demonstrated underestimate in AOD and underestimate in absorption in the model (MOZEX) over southern Africa (Ginoux et al., 2006; Magi et al., 2009), for use in the remaining three experiments, we combined observations of column-integrated AOD and SSA from AERONET and the *EP*-TOMS instrument (Torres et al., 2005) into monthly-mean gridded maps (Fig. 1a–b). We chose to use data from *EP*-TOMS because, to our knowledge, it and its successor OMI are the only observational

Biomass burning aerosol climate impacts

C. A. Randles and
V. Ramaswamy

Title Page

Abstract

Introduction

Conclusions

References

Tables

Figures

⏪

⏩

◀

▶

Back

Close

Full Screen / Esc

Printer-friendly Version

Interactive Discussion

**Biomass burning
aerosol climate
impacts**C. A. Randles and
V. Ramaswamy

Title Page

Abstract

Introduction

Conclusions

References

Tables

Figures

⏪

⏩

◀

▶

Back

Close

Full Screen / Esc

Printer-friendly Version

Interactive Discussion

datasets that provide horizontal distributions of *both* column-integrated and AOD and SSA over both land and ocean. AOD and SSA are derived from *EP-TOMS* retrievals using the near-UV retrieval method (Torres et al., 1998, 2002, 2005). This method uses the ratio of backscattered radiances at two measured UV wavelengths (330 and 380 nm) in an inversion procedure that employs a pre-compiled set of look-up tables (LUTs). The LUTs are generated using a radiative transfer code that assumes aerosol models based on a combination of spectral and geographical location considerations (based on emission characteristics) to determine column-integrated AOD and SSA. Retrieved AOD and SSA, with errors of $\pm 30\%$ and ± 0.03 , respectively, are reported at 380 nm and interpolated to 500 nm using the LUTs. Sources of uncertainty in the *EP-TOMS* retrievals include the assumed aerosol vertical distribution and sub-pixel cloud contamination effects resulting from the wide field of view ($40\times 40\text{ km}^2$ at nadir and as large as $200\times 200\text{ km}^2$ at extreme off-nadir viewing geometry). The largest overestimates by *EP-TOMS* occur when extinction optical depths are below 0.2 because the coarse resolution of the *EP-TOMS* product makes it difficult to resolve small-scale variability. However, the advantages of the near-UV retrieval method are the ability to retrieve aerosol properties over most terrestrial surfaces including deserts and a low sensitivity to particle shape (Torres et al., 2002). During SAFARI 2000, Torres et al. (2005) performed an extensive validation of *EP-TOMS* relative to AERONET and found that column-integrated AOD and SSA were generally within the observational uncertainty of AERONET.

In constructing the maps (Fig. 1a–b), daily-mean retrievals of AOD and SSA from *EP-TOMS* were aggregated to the model grid. Then, if a grid-box did not contain an *EP-TOMS* retrieval for a particular day and if the grid-box was co-located with one of 18 AERONET sites in southern Africa during 2000 (see supplemental material for a listing of sites used, <http://www.atmos-chem-phys-discuss.net/10/9731/2010/acpd-10-9731-2010-supplement.pdf>), we assigned the grid box the daily-averaged Level 2.0, Version 2.0 AERONET observation of AOD and SSA at 500 nm, if available. Grid-boxes with missing data were then linearly interpolated from nearest-neighbor

grid-boxes. Daily-mean gridded maps were then averaged to monthly-mean maps. It is important to emphasize that in this sensitivity study, these maps are used only as a guide to design experiments that are more similar to available observations than MOZEX. Because our aim in using these maps is simply to help define a reasonable parameter space for AOD and SSA, it is beyond the scope of this study to do a detailed comparison of *EP-TOMS* and *AERONET* retrievals of AOD and SSA, as was done in Torres et al. (2005).

Figure 1 compares the 500 nm ASO column-integrated and area-averaged (3° N–37° S, 19° E–50° W) AOD and SSA using the observations (Fig. 1a–b) and the four experiments (Fig. 1c–f). SFC, TOA, and ATM all-sky (cloudy plus clear) radiative forcing efficiencies, which are defined as the radiative forcing per unit AOD, are shown in Fig. 1g. In experiment HIGHEX, BC and OC distributions from MOZART-2 are scaled-up in proportion below ~4 km over southern Africa so that column-integrated AOD roughly agrees with our observationally-based map (Fig. 1a) while the SSA is the same as in MOZEX (Fig. 1d). We only alter the bb aerosol distributions below ~4 km because boundary-layer (BL) height in southern Africa typically reaches this height in the early afternoon, and during SAFARI 2000, bb aerosol tended to be well mixed in the BL over land due to strong dry convection (Haywood et al., 2003). We note that in constructing HIGHEX and the remaining two experiments, the humidity profile from MOZEX was used to approximate the humidified optical properties of OC and SO₄ before adjusting the (dry) masses of OC and BC to obtain the column-integrated optical properties of the observationally-based maps. This may lead to an overestimation or underestimation of AOD compared to the observations if the model relative humidity in a given sensitivity experiment is lower or higher than in MOZEX, respectively. However, since our purpose in this sensitivity study is to try and bound the real world, it is not necessary that we precisely mimic observations, which are also very uncertain.

In experiment SSAEX, OC and BC are also scaled up below ~4 km to agree roughly with the AOD in Fig. 1a. In addition, the proportion of OC to BC below ~4 km is altered so that the column-integrated SSA is similar to the observations (Fig. 1b). Our final

**Biomass burning
aerosol climate
impacts**C. A. Randles and
V. Ramaswamy

Title Page

Abstract

Introduction

Conclusions

References

Tables

Figures

◀

▶

◀

▶

Back

Close

Full Screen / Esc

Printer-friendly Version

Interactive Discussion

experiment WHITE has the same AOD as HIGHEX and SSAEX (Fig. 1e), but the optical properties of BC and OC are artificially set to be scattering-only such that $SSA \sim 1$ (deviation from 1 due to presence of some absorbing dust; not shown). The main aim for this hypothetical experiment is to flush out the contrasts with the experiments with increased absorbing bb aerosols (MOZEX, HIGHEX, SSAEX) and thus more clearly delineate their role.

Figure 2 shows a comparison of modeled and observed climatological AOD at four AERONET stations. In MOZEX, biomass burning tends to peak in October rather than in September as observed. By applying the scaling as described, we improve agreement between the model and observations of AOD, particularly in the biomass burning season. However, we likely overestimate the SSA (underestimate absorption) in our bounding experiment SSAEX ($SSA = 0.9$) since the SAFARI-2000 campaign-average SSA was estimated at 0.85 ± 0.03 (Leahy et al., 2007). Total BC mass from MOZEX is roughly doubled in the other three experiments, and OC mass increases by roughly a factor of 2.5 (see supplemental material for horizontal and vertical distributions of BC and OC).

3 Results

In the following analysis, we focus on differences between the response of each experiment and the CTRL experiment over southern Africa ($3^\circ \text{N} - 37^\circ \text{S}$, $19^\circ \text{E} - 50^\circ \text{W}$) for ASO (i.e. $\Delta = \text{EXPERIMENT} - \text{CTRL}$). In contrast to Figs. 1 and 2, which evaluated the representativeness of the column-integrated aerosol optical properties against observations, here we evaluate the sensitivity of the climate system to the bb aerosol specifications. Because only the bb aerosol forcing differs between a given experiment and CTRL, analyzing these differences yields the response of the model to bb forcing only, where here we have assumed that the bb aerosol forcing is dominated by its carbonaceous (BC plus OC) component. Our equilibrium experiments are neither appropriate to gain insight into the actual time evolution of the 20th century climate response to bb aerosol

Biomass burning aerosol climate impacts

C. A. Randles and
V. Ramaswamy

Title Page

Abstract

Introduction

Conclusions

References

Tables

Figures

⏪

⏩

◀

▶

Back

Close

Full Screen / Esc

Printer-friendly Version

Interactive Discussion

radiative forcing nor can they predict real changes in the African climate. Our aim is to compare and contrast the range of climate response possible given a realistic range in bb aerosol radiative forcing. Since we are attempting to extract the influences of aerosols alone on observed climate changes, isolated from additional forcing factors such as GHGs, land-use change, and SSTs that are present in the real climate, we cannot make direct comparisons to observational data.

Recall from Fig. 1g that despite slight differences in their horizontal (Fig. 1d, f) and vertical distributions (see supplemental material) of aerosol optical properties, the forcing efficiencies for HIGHEX and SSAEX are quite similar on an area-averaged basis; as a result, the climate response is also similar for these two experiments. Abel et al. (2005) conducted an extensive sensitivity study of direct aerosol forcing over southern Africa, and the TOA and SFC forcing for SSAEX and HIGHEX is generally consistent with their forcing estimates for highly absorbing bb haze (SSA = 0.84). Figure 1h shows the change, relative to CTRL, in the ASO area-average components of the land surface energy balance for each experiment. Positive (negative) terms warm (cool) the surface. The land surface energy balance is given by:

$$S + F + LE + H \approx 0 \quad (1)$$

where S is the net (down minus up) solar (shortwave) heat flux at the surface, F is the net longwave heat flux, and LE and H are the net latent and sensible heat fluxes, respectively. Note that, while the balance in (1) is obtained for the global, annual mean (not shown), there is a small residual for ASO. Absorbing bb burning aerosols (MOZEX, HIGHEX, SSAEX) decrease shortwave flux to the surface relative to CTRL, and increased (less negative) sensible heating rather than latent heating compensates this surface cooling due to the dryness of the season (Abel et al., 2005). In contrast, when scattering-only aerosols increase (WHITE), area-average shortwave surface heating decreases less relative to the other experiments due to decreases in cloud amount (see Fig. 3), and latent heating occurs as evaporation decreases (not shown).

**Biomass burning
aerosol climate
impacts**C. A. Randles and
V. Ramaswamy

Title Page

Abstract

Introduction

Conclusions

References

Tables

Figures

◀

▶

◀

▶

Back

Close

Full Screen / Esc

Printer-friendly Version

Interactive Discussion

**Biomass burning
aerosol climate
impacts**C. A. Randles and
V. Ramaswamy

Title Page

Abstract

Introduction

Conclusions

References

Tables

Figures

◀

▶

◀

▶

Back

Close

Full Screen / Esc

Printer-friendly Version

Interactive Discussion

Figure 3a–d shows the change in surface air temperature (ΔT_{sat}) and the change in low-level cloud amount for each experiment relative to CTRL (see supplemental material for T_{sat} and low-level cloud distributions in CTRL). BB aerosol backscattering and absorption reduce shortwave radiation at the surface, and significant cooling is observed in central Africa ($\sim 0\text{--}15^\circ\text{S}$ over land). The cooling pattern observed in MOZEX, SSAEX, and HIGHEX is spatially coherent with the pattern of bb aerosol AOD (Fig. 1c, e), and both higher AOD and cloud amount increases in SSAEX and HIGHEX contribute to stronger surface air cooling over land compared to MOZEX. Conversely, decreased cloud amount in equatorial Africa in WHITE contributes to surface warming in this region despite high bb aerosol AOD. Over the ocean, there is little change in surface air temperature for all experiments since SSTs are the same as in the CTRL experiment. However, when absorbing bb aerosol is increased, clouds tend to decrease over the ocean north of 10°S (where bb burning AOD is the highest) and decrease to the south ($10^\circ\text{S}\text{--}15^\circ\text{S}$). The zonally averaged air temperature change (not shown) indicates that the troposphere generally warms in MOZEX, HIGHEX, and SSAEX, though there is cooling near the land surface in the region with the highest bb aerosol AOD ($\sim 0\text{--}15^\circ\text{S}$), indicating an increase in low-level thermodynamic stability. The atmosphere generally cools throughout in WHITE, though there is some near-surface warming over land north of 10°S , likely due to sensible and latent warming.

Figure 3e–h shows the change in precipitation (ΔP) and the change in column-integrated precipitable water (ΔWVP) for each experiment relative to CTRL (see supplemental material for ASO precipitation (P) and WVP for CTRL). Rainfall changes are small and generally not significant, except in WHITE where significant decreases occur in central equatorial Africa. We note that the stronger increases in absorbing bb aerosol in SSAEX and HIGHEX are associated with small regions of precipitation increase in central equatorial Africa. The rainfall anomaly patterns induced by bb aerosol over central Africa are consistent with the patterns of column-integrated water vapor, which are more significant than the precipitation changes. Our cloud and water vapor changes in HIGHEX and SSAEX are consistent with a negative semi-direct effect,

which can be attained when absorbing aerosol are located both within and above the boundary layer (Johnson et al., 2004).

During the dry season, a semi-permanent continental-scale subtropical anticyclone induces large-scale subsidence over southern Africa (Garstang et al., 1996). The ASO change in sea-level pressure (SLP) and 850-hPa winds relative to CTRL is shown in Fig. 4a–d. Increasing absorbing bb aerosol tends to increase low-level flow from the equatorial Atlantic towards the west African coast, and SLP increases over land when AOD is high (HIGHEX and SSAEX), consistent with the findings of Roeckner et al., (2006) and RR08. However, when there are strong increases in scattering aerosols only, the 850-hPa wind anomaly is in the same sense as the CTRL experiment (i.e. from land to ocean; see supplemental material).

The zonally-averaged meridional circulation anomalies (Fig. 4e–h) indicate increased upward motion coincident with regions of increased absorbing bb aerosol (~ 0 – 15° S). This rising motion, along with the anomalous low-level circulation and subsequent low-level convergence (not shown) contribute to the simulated increases in column-integrated water, precipitation, and clouds over land in SSAEX and HIGHEX (and, to a lesser extent in MOZEX). There are much weaker increases in vertical motion in equatorial Africa in WHITE, and increasing aerosol scattering alone tends to spin-down the hydrologic cycle in southern Africa. Table 2 summarizes the area-average changes in surface air temperature and the hydrologic cycle examined in this study.

4 Discussion and conclusions

Motivated by the variability in the observations of aerosol optical properties and the wide range in the estimates of aerosol radiative forcing over southern Africa, simulations are carried out in the GFDL AM2-LM2 GCM to test the climate sensitivity to a range of biomass burning aerosol radiative forcing. The modeled radiative forcing by absorbing bb aerosol reduces the solar flux to the surface, heats the atmosphere, and tends to stabilize the troposphere below the aerosol layer while increasing the surface

Biomass burning aerosol climate impacts

C. A. Randles and
V. Ramaswamy

Title Page

Abstract

Introduction

Conclusions

References

Tables

Figures

⏪

⏩

◀

▶

Back

Close

Full Screen / Esc

Printer-friendly Version

Interactive Discussion

**Biomass burning
aerosol climate
impacts**C. A. Randles and
V. Ramaswamy

Title Page

Abstract

Introduction

Conclusions

References

Tables

Figures

⏪

⏩

◀

▶

Back

Close

Full Screen / Esc

Printer-friendly Version

Interactive Discussion

pressure over land. Over the ocean, however, the cooling tendency of this reduced solar flux is not realized (due to prescribed SSTs in this case, or, alternatively due to a lagged ocean response), though bb aerosol absorption still exerts a warming tendency on the atmosphere. A thermally-driven anomalous circulation from the Atlantic towards the west African coast results, and warm, moist air is lofted above the continent, increasing clouds, column-integrated water vapor, and, to a lesser extent, precipitation in the main bb aerosol region (~ 0 – 15° S).

We also consider a case in which bb aerosols are completely scattering, and this experiment represents a hypothetical case, at least in the context of the contemporary atmosphere. This experiment serves to flush out the contrasts in the response to scattering aerosols, which only exert a radiative cooling tendency on the surface, with the response to absorbing aerosols, which simultaneously cool the surface and warm the atmosphere. Our results show that increased aerosol scattering in the absence of increased absorption tends to cool the atmosphere over southern Africa and enhance subsidence over the region. The resulting decreases in cloud amount offset some of the surface cooling tendency associated with high AOD, and the hydrologic cycle over southern Africa tends to spin-down compared to increasing absorbing bb aerosol.

In this study, SSTs were prescribed as an important first step to isolate and examine only the affects of aerosols on southern Africa without the complexity of a fully coupled ocean-atmosphere model. It is important to note that if SST changes due to aerosol surface cooling were to yield strong feedbacks, particularly with regard to clouds, the effects of aerosols on the hydrologic cycle could become more complicated. For example, cooler SSTs due to increased aerosol loadings may contribute to decreases in surface convergence (e.g. Hackert and Hastenrath, 1986) and convection; however, the SST response is expected to lag aerosol forcing (e.g. Ramanathan and Carmichael, 2008). Furthermore, our findings may be sensitive to the GCM convective parameterization (e.g. Chakraborty et al., 2004), as we have shown that dynamically driven cloud changes can reinforce or eclipse aerosol effects, particularly on surface air temperature. Inclusion of aerosol indirect effects would also complicate the

relationship between aerosols and cloud amount and their associated surface solar flux changes. We also neglected the feedback of the hydrologic cycle on aerosol distributions; however, we expect this to be rather small during the dry season studied here. We reiterate that our results for increased absorbing bb aerosol (HIGHEX, SSAEX) are consistent with those Roeckner et al. (2006), which used a fully coupled atmosphere-ocean model, interactive aerosols, and the first aerosol indirect effect. Our findings with regard to the effects of bb aerosols on the hydrologic cycle are also broadly consistent with the findings of Ott et al. (2010), which studied the climate effects of biomass burning in the Indonesian region. We also note that our most absorbing case (SSAEX) likely underestimates aerosol absorption over southern Africa; stronger aerosol absorption would likely strengthen the dynamic and hydrodynamic responses observed in this experiment. Despite these caveats, our study supports the primary conclusion that radiative forcing from biomass burning aerosol is an important player in climate change over southern Africa. In particular, it is clear that the hydrologic cycle over the continent is sensitive to the total amount of aerosol absorption.

Acknowledgements. The authors thank Paul Ginoux and Hiram Levy II for thoughtful comments on the manuscript. We thank Omar Torres for providing daily *EP*-TOMS retrievals of AOD and SSA for 2000 and the AERONET investigators and their staff for establishing and maintaining the 18 sites used in this investigation. CAR acknowledges funding from the DOE Graduate Research Environmental Fellowship and the Princeton AOS program.

References

- Abel, S. J., Highwood, E. J., Haywood, J. M., and Stringer, M. A.: The direct radiative effect of biomass burning aerosols over southern Africa, *Atmos. Chem. Phys.*, 5, 1999–2018, 2005, <http://www.atmos-chem-phys.net/5/1999/2005/>.
- Anderson, J. et al.: The new GFDL global atmosphere and land model AM2-LM2: Evaluation with prescribed SST simulations, *J. Climate*, 17, 4641–4673, 2004.
- Chakraborty, A., Satheesh, S. K., Nanjundiah, R. S., and Srinivasan, J.: Impact of absorbing aerosols on the simulation of climate over the Indian region in an atmospheric general circu-

Biomass burning aerosol climate impacts

C. A. Randles and
V. Ramaswamy

Title Page

Abstract

Introduction

Conclusions

References

Tables

Figures

⏪

⏩

◀

▶

Back

Close

Full Screen / Esc

Printer-friendly Version

Interactive Discussion



lation model, *Ann. Geophys.*, 22, 1421–1434, 2004,

<http://www.ann-geophys.net/22/1421/2004/>.

Garstang, M., Tyson, P. D., Swap, R., Edwards, M., Kållbert, P., and Lindesay, J. A.: Horizontal and vertical transport of air over southern Africa, *J. Geophys. Res.*, 101, 23721–23736, 1996.

Ginoux, P., Horowitz, L. W., Ramaswamy, V., Geogdzhayev, I. V., Holben, B. N., Stenchikov, G., and Tie, X.: Evaluation of aerosol distribution and optical depth in the Geophysical Fluid Dynamics Laboratory coupled model CM2.1 for present climate, *J. Geophys. Res.*, 111, D22210, doi:10.1029/2005JD006707, 2006.

Hackert, E. C. and Hastenrath, S.: Mechanisms of Java rainfall anomalies, *Mon. Weather Rev.*, 114, 745–757, 1986.

Haywood, J. M. and Ramaswamy, V.: Global Sensitivity studies of the direct radiative forcing due to anthropogenic sulfate and black carbon aerosols, *J. Geophys. Res.*, 103, D6, 6043–6058, 1998.

Haywood, J. M., Ramaswamy, V., and Soden, B. J.: Tropospheric aerosol climate forcing in clear-sky satellite observations over the oceans, *Science*, 283, 5406, 1299–1303, 1999.

Haywood, J. M., Osborne, S. R., Francis, P. N., Keil, A., Formenti, P., Andreae, M. O., and Kaye, P. H.: The mean physical and optical properties of regional haze dominated by biomass burning aerosol measured from the C-130 aircraft during SAFARI 2000, *J. Geophys. Res.*, 108, D13, 8473, doi:10.1029/2002JD002226, 2003.

Holben, B. et al.: An emerging ground-based aerosol climatology: Aerosol optical depth from AERONET, *J. Geophys. Res.*, 106, D11, 12067–12097, 2001.

Horowitz, L.: Past, present, and future concentrations of tropospheric ozone and aerosols: Methodology, ozone evaluation, and sensitivity to aerosol wet removal, *J. Geophys. Res.*, 111, D22211, doi:10.1029/2005JD006937, 2006.

Johnson, B. T., Shine, K. P., and Forster, P. M.: The semi-direct aerosol effect: Impact of absorbing aerosols on marine stratocumulus, *QJRM*, 130, 599, 1407–1422, 2004.

Kaufman, Y. J., Tanre, D., Remer, L., Vermonte, E., Chu, A., and Holben, B. N.: Remote sensing of tropospheric aerosol over the land using dark targets and dynamic aerosol models, *J. Geophys. Res.*, 102, 17051–17067, 1997.

Keil, A. and Haywood, J. M.: Solar radiative forcing by biomass burning aerosol particles during SAFARI 2000: A case study based on measured aerosol and cloud properties, *J. Geophys. Res.*, 108, D13, 8467, doi:10.1029/2002JD002315, 2003.

**Biomass burning
aerosol climate
impacts**

C. A. Randles and
V. Ramaswamy

Title Page

Abstract

Introduction

Conclusions

References

Tables

Figures

◀

▶

◀

▶

Back

Close

Full Screen / Esc

Printer-friendly Version

Interactive Discussion

**Biomass burning
aerosol climate
impacts**C. A. Randles and
V. Ramaswamy[Title Page](#)[Abstract](#)[Introduction](#)[Conclusions](#)[References](#)[Tables](#)[Figures](#)[⏪](#)[⏩](#)[◀](#)[▶](#)[Back](#)[Close](#)[Full Screen / Esc](#)[Printer-friendly Version](#)[Interactive Discussion](#)

- Lau, K. M., Kim, M. K., and Kim, K. M.: Asian summer monsoon anomalies induced by aerosol direct forcing: The role of the Tibetan Plateau, *Clim. Dynamics*, 26(7–8), 855–864, 2006.
- Leahy, L. V., Anderson, T. L., Eck, T. F., and Bergstrom, R. W.: A Synthesis of biomass burning aerosol over southern Africa during SAFARI 2000, *Geophys. Res. Lett.*, 34, L12814, doi:10.1029/2007GL029697, 2007.
- Magi, B. I., Ginoux, P., Ming, Y., and Ramaswamy, V.: Evaluation of tropical and extratropical Southern Hemisphere African aerosol properties simulated by a climate model, *J. Geophys. Res.*, 114, D14204, doi:10.1029/2008JD011128, 2009.
- Magi, B. I. and Hobbs, P. V.: Hobbs: Effects of humidity on aerosols in southern Africa during the biomass burning season, *J. Geophys. Res.*, 108(D13), 8495, doi:10.1029/2002JD002144, 2003.
- Menon, S., Hansen, J., Nazarenko, L., and Luo, Y.: Climate effects of black carbon aerosols in China and India, *Science*, 297, 2250–2253, 2002.
- Ming, Y., Ramaswamy, V., Ginoux, P. A., and Horowitz, L. H.: Direct radiative forcing of anthropogenic organic aerosol, *J. Geophys. Res.*, 110, D20208, doi:10.1029/2004JD005573, 2005.
- Myhre, G., Bernsten, T. K., Haywood, J. M., Sundet, J. K., Holben, B. N., Johnsrud, M., and Stordal, F.: Modeling the solar radiative impact of aerosols from biomass burning during the Southern African Regional Science Initiative (SAFARI-2000) experiment, *J. Geophys. Res.*, 108(D13), 8501, doi:10.1029/2002JD002313, 2003.
- Ott, L., Duncan, B., Pawson, S., Colarco, P. R., Chin, M., Randles, C., Diehl, T., and Nielsen, E.: The influence of the 2006 Indonesian biomass burning aerosols on tropical dynamics studied with the GEOS-5 AGCM, *J. Geophys. Res.*, doi:10.1029/2009JD013181, in press., 2010.
- Paeth, H. and Feichter, J.: Greenhouse-gas versus aerosol forcing and African climate response, *Clim. Dynam.*, 26, 35–54, 2006.
- Ramanathan V. and Carmichael, G.: Global and regional climate changes due to black carbon, *Nat. Geosci.*, 1, 221–227, 2008.
- Randles, C. A. and Ramaswamy, V.: Absorbing aerosols over Asia: A GFDL general circulation model sensitivity study of model response to aerosol optical depth and aerosol absorption, *J. Geophys. Res.*, 113, D21203, doi:10.1029/2008JD010140, 2008.
- Reynolds, R. W., Rayner, N. A., Smith, T. M., Stockes, D. C., and Wang, W.: An improved in situ and satellite SST analysis for climate, *J. Climate*, 15, 1609–1625, 2002.

Roeckner, E., Stier, P., Feichter, J., Kloster, S., Esch, M., and Fischer-Bruns, L.: Impact of carbonaceous aerosol emissions on regional climate change, *Clim. Dynam.*, 27, 552–571, 2006.

Solomon S. et al.: Technical Summary Contribution of Working Group 1 to the 4th Assessment Report of the Intergovernmental Panel on Climate Change, in: *Climate Change 2007: The Physical Science Basis*, Cambridge University Press, New York, 21–87, 2007.

Torres, O., Bhartia, P. K., Herman, J. R., Ahmad, Z., and Gleason, J.: Derivation of aerosol properties from satellite measurements of backscattered ultraviolet radiation: Theoretical basis, *J. Geophys. Res.*, 103, 17099–17110, 1998.

Torres, O., Bhartia, P. K., Herman, J. R., Sinyuk, A., Ginoux, P., and Holben, B.: A long-term record of aerosol optical depth from TOMS observations and comparison to AERONET measurements, *J. Atmos. Science*, 59, 398–413, 2002.

Torres, O., Bhartia, P. K., Sinyuk, a., Welton, E. J., and Holben, B.: Total Ozone Mapping Spectrometer measurements of aerosol absorption from space: Comparison to SAFARI 2000 ground-based observations, *J. Geophys. Res.*, 110, D10S18, doi:10.1029/2004JD004611, 2005.

**Biomass burning
aerosol climate
impacts**

C. A. Randles and
V. Ramaswamy

Title Page

Abstract

Introduction

Conclusions

References

Tables

Figures

◀

▶

◀

▶

Back

Close

Full Screen / Esc

Printer-friendly Version

Interactive Discussion

Biomass burning aerosol climate impacts

C. A. Randles and
V. Ramaswamy

Table 1. Experimental Design. All experiments have the same natural (sea salt plus dust) and sulfate (SO_4) distributions from MOZART-2 (Horowitz, 2006). Experiments differ based solely on the prescription of OC and BC distributions. All other forcing agents (e.g. long-lived greenhouse gases, prescribed observed sea surface temperatures) are held constant. Differing an experiment with respect to the CTRL case indicates the response of the model to biomass burning aerosol forcing.

Experiment	Natural Aerosols and SO_4	Biomass Burning (BC and OC) aerosols
CTRL	MOZART-2 Y2000	None
MOZEX	MOZART-2 Y2000	MOZART-2 Y2000
HIGHEX	MOZART-2 Y2000	MOZART-2 Y2000 adjusted below ~ 4 km to mimic total aerosol AOD in Fig. 1a; same SSA as MOZEX
SSAEX	MOZART-2 Y2000	MOZART-2 Y2000 adjusted below ~ 4 km to mimic total aerosol AOD and SSA in Figs. 1a and b.
WHITE	MOZART-2 Y2000	Same as HIGHEX but optical properties of OC and BC treated as dry sulfate.

[Title Page](#)
[Abstract](#)
[Introduction](#)
[Conclusions](#)
[References](#)
[Tables](#)
[Figures](#)




[Back](#)
[Close](#)
[Full Screen / Esc](#)
[Printer-friendly Version](#)
[Interactive Discussion](#)

Biomass burning aerosol climate impacts

C. A. Randles and
V. Ramaswamy

Table 2. Summary of ASO area-weighted average (3° N– 37° S, 19° E– 50° W) change in surface air temperature (T_{sat}), precipitation minus evaporation (P-E; [mm d^{-1}]) column-integrated precipitable water (WVP) [mm], and low-level clouds [%]. Land-only averages are given with land plus ocean averages in parenthesis

Change Relative to CTRL	MOZEX	HIGHEX	SSAEX	WHITE
ΔT_{sat} [K]	-0.12 (-0.08)	-0.27 (-0.15)	-0.35 (-0.18)	-0.27 (-0.16)
$\Delta(\text{P-E})$ [mm d^{-1}]	+0.02 (+0.04)	+0.05 (+0.08)	+0.05 (+0.08)	-0.1 (-0.07)
Δ Precipitable Water [mm]	0 (+0.1)	+0.2 (+0.3)	+0.2 (+0.2)	-1.2 (-0.9)
Δ Low Clouds [%]	+0.4 (+0.4)	+0.7 (+0.1)	+0.7 (-0.3)	-1.0 (-0.9)

[Title Page](#)
[Abstract](#)
[Introduction](#)
[Conclusions](#)
[References](#)
[Tables](#)
[Figures](#)
[Back](#)
[Close](#)
[Full Screen / Esc](#)
[Printer-friendly Version](#)
[Interactive Discussion](#)

Biomass burning aerosol climate impacts

C. A. Randles and
V. Ramaswamy

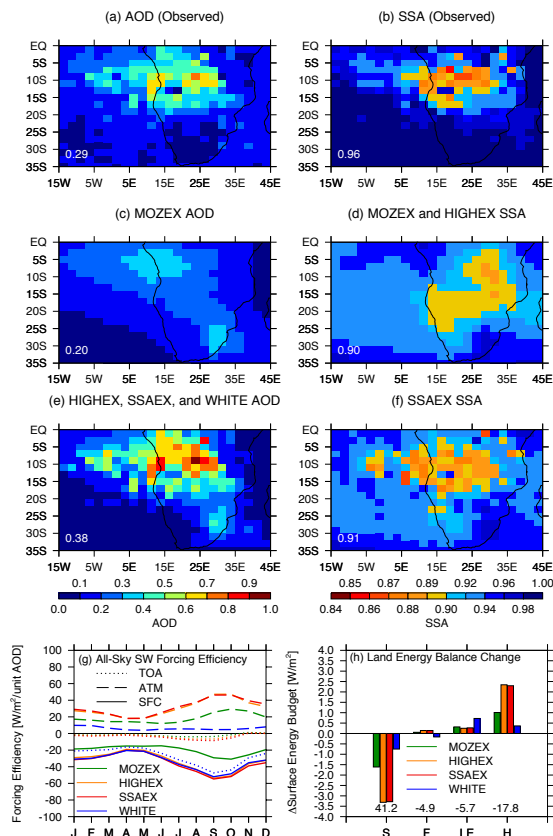


Fig. 1. Column-integrated ASO 500 nm **(a)** AOD and **(b)** SSA based on AERONET and *EP*-TOMS observations. **(c)** AOD for MOZEX. **(d)** SSA shared for MOZEX and HIGEX **(e)** AOD shared for SSAEX, HIGEX and WHITE based on (a). **(f)** SSA for SSAEX based on (b). Area-averaged (3° N– 37° S, 19° E– 50° W) values are printed in lower left of each panel. **(g)** Monthly-mean area-averaged SFC, ATM, and TOA forcing efficiency [W m^{-2} per unit AOD] where $\text{TOA} = \text{SFC} + \text{ATM}$. **(h)** ASO area-average equilibrium change in *S*, *F*, *LE*, and *H* fluxes at the surface relative to CTRL from Eq. (1) [W m^{-2}]; positive (negative) changes warm (cool) the surface. Area-average values for CTRL are listed along the lower portion of panel (h).

[Title Page](#)
[Abstract](#)
[Introduction](#)
[Conclusions](#)
[References](#)
[Tables](#)
[Figures](#)
[◀](#)
[▶](#)
[◀](#)
[▶](#)
[Back](#)
[Close](#)
[Full Screen / Esc](#)
[Printer-friendly Version](#)
[Interactive Discussion](#)

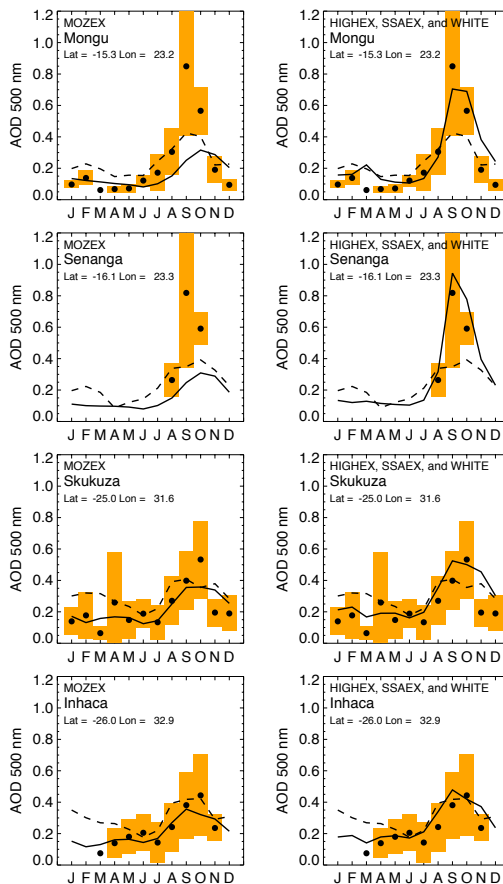
**Biomass burning
aerosol climate
impacts**C. A. Randles and
V. Ramaswamy

Fig. 2. Comparison of simulated (solid black lines) AOD to monthly-mean climatological observations from AERONET (black dots; orange bars are standard deviation) and MODIS retrievals (dashed lines; 2002–2004 average). Left column is for MOZEX and right column is for experiments with OC and BC mass adjusted to match observationally-based maps of column-integrated optical properties (i.e. HIGHEX, SSAEX, and WHITE). Mongu and Senanga lie in the primary biomass burning region ($\sim 0\text{--}18^\circ\text{S}$) during the dry season (ASO).

[Title Page](#)[Abstract](#)[Introduction](#)[Conclusions](#)[References](#)[Tables](#)[Figures](#)[⏪](#)[⏩](#)[◀](#)[▶](#)[Back](#)[Close](#)[Full Screen / Esc](#)[Printer-friendly Version](#)[Interactive Discussion](#)

Biomass burning
aerosol climate
impactsC. A. Randles and
V. Ramaswamy

Title Page

Abstract

Introduction

Conclusions

References

Tables

Figures

◀

▶

◀

▶

Back

Close

Full Screen / Esc

Printer-friendly Version

Interactive Discussion

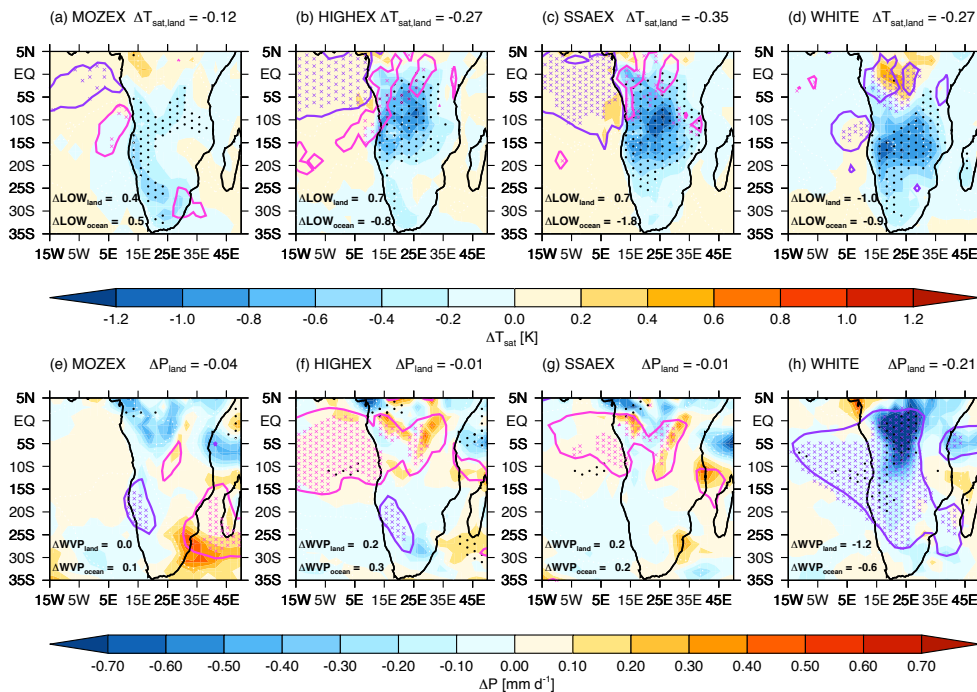


Fig. 3. ASO surface air temperature change relative to CTRL (ΔT_{sat} ; [K]) (shaded) for (a) MOZEX, (b) HIGHEX, (c) SSAEX, and (d) WHITE with black stippling indicating that changes above 90% are significant. Overlain pink (purple) contours are increased (decreased) low-level cloud above (below) 2.5% with pink (purple) crosses denoting 90% significance. See supplemental material for T_{sat} and low-level cloud distributions from CTRL. (e) Change in total precipitation relative to CTRL (ΔP ; [mm d⁻¹]) (shaded) for (e) MOZEX, (f) HIGHEX, (g) SSAEX, and (h) WHITE with black stippling indicating 90% significance. Overlain pink (purple) contours are increased (decreased) column-integrated precipitable water (ΔWVP) above (below) 0.5 mm with pink (purple) crosses denoting 90% significance. See supplemental material for P and column-integrated precipitable water from CTRL.

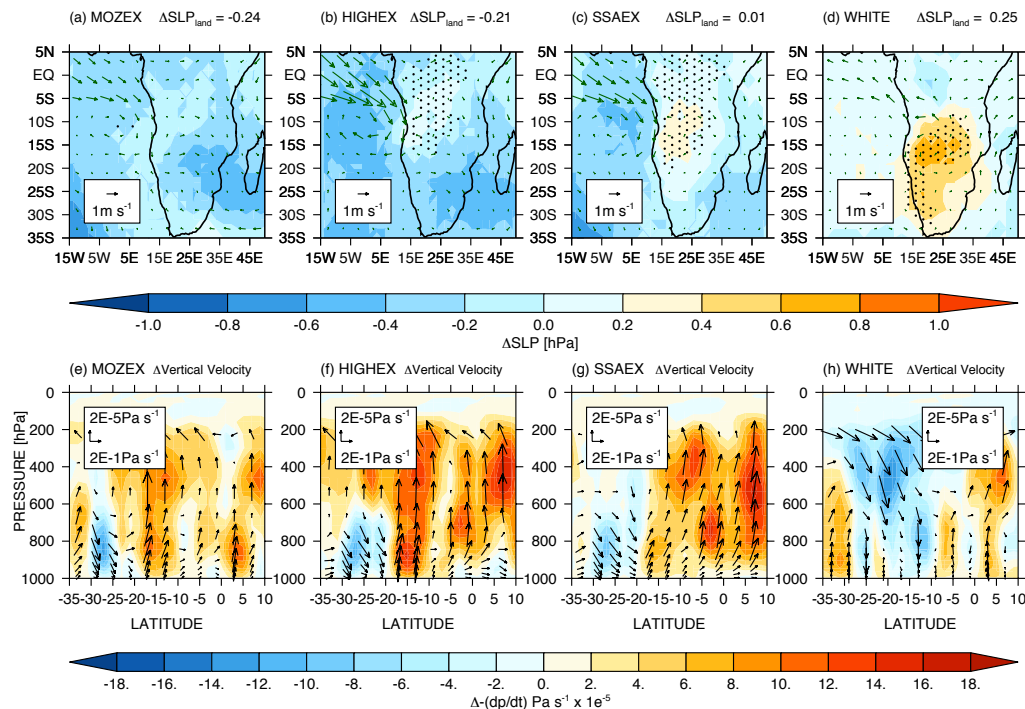
Biomass burning
aerosol climate
impactsC. A. Randles and
V. Ramaswamy

Fig. 4. ASO change in sea level pressure (ΔSLP) relative to CTRL [hPa] for (a) MOZEX, (b) HIGHEX, (c) SSAEX, and (d) WHITE overlain with 850-hPa wind anomaly relative to CTRL; black stippling represents ΔSLP above 90% significant. Zonally averaged (0–50° E) change in vertical velocity ($-\text{dp}/\text{dt}$) relative to CTRL [$\text{Pa s}^{-1} \times 10^{-5}$] for (e) MOZEX, (f) HIGHEX, (g) SSAEX, and (h) WHITE overlain with meridional circulation change; note red (blue) shading indicates increased upward motion (relative subsidence). See supplemental material for the CTRL case SLP and 850-hPa wind circulation.

Title Page

Abstract

Introduction

Conclusions

References

Tables

Figures

◀

▶

◀

▶

Back

Close

Full Screen / Esc

Printer-friendly Version

Interactive Discussion